한국지반공학회논문집 제16권 제4호 2000년 8월 PP 183 ~190

Finite Element Analysis of Piezocone Test I

피에조콘 시험의 유한요소 해석 I

Kim, Dae-Kyu* 김 대 규

요 지

본 연구에서는 피에조콘 시험의 유한요소 해석을 점탄소성 bounding surface 구성모델과 large displacement large deformation 개념을 이용하여 수행하였다. 이에 따라 구성모델, 가상일의 방정식 및 관련 유한요소 식 등을 Updated Lagrangian reference frame에서 formulation 하였으며 지반의 거동은 theory of mixtures를 통하여 설명하였다. Theory of mixtures 역시 Updated Lagrangian reference frame에서 formulation하였다. 구성모델 중 점성부분이 전체 formulation 과정에 중요한 영향을 미친다는 사실이 고찰되었다. 유한요소 해석의 결과는 실내에서 실시한 대형 모델시험의 결과와 비교, 분석하였다. Formulation 과정은 'Ⅰ', 결과는 'Ⅱ'에서 설명된다.

Abstract

In this research, the finite element analysis of piezocone penetration and dissipation tests have been conducted using the anisotropic elastoplastic-viscoplastic bounding surface model in the Updated Lagrangian reference frame for the large deformation and finite strain nature of piezocone penetration. Accordingly, virtual work equation and corresponding finite element equations have been reformulated. Theory of mixtures has been incorporated to explain the behavior of the soil. It has been observed that the viscoplastic part of the soil model affected the whole formulation. The results of the finite element analysis have been compared and investigated with the experimental results. The formulations and the results are described in part 'Ⅰ' and part 'Ⅱ', respectively.

Keywords : Bounding surface model, Piezocone, Updated lagrangian formulation

1. Introduction

Finite element method, besides the methods based on semi-empirical approach, bearing capacity models, cavity expansion theory, and strain path method, has been used and become a important method to analyze the complex cone penetration mechanism considering many influencing factors (Deborst and Vermeer, 1984; Kiousis, et al., 1988; Sandven, 1990; Teh and Houlsby, 1991; Van den Berg, et al., 1994; Abu-Farsakh, et al., 1997). The previous studies have used elastoplastic soil models; however, elastoplasticity alone can not account for time dependent behavior such as strain rate effect that is one of the important factors affecting the cone penetration mechanism. Prediction of time dependent behavior requires the use of viscoplasticity.

In this research, the anisotropic elastoplastic-viscoplastic bounding surface model (Al-Shamrani and Sture, 1994) was formulated in the Updated Lagrangian frame to consider anisotropy and strain rate effects as well as large displacement and finite strain nature of cone penetration mechanism. Theory of mixtures (Prevost, 1980; Abu-Farsakh, et al., 1997) was incorporated to explain the soil behavior.

*정회원, 고려대학교 방재과학기술연구센터 선임연구원

Virtual work equation and corresponding finite element equations have been formulated in the Updated Lagrangian frame and implemented into a finite element program. The results of the finite element analysis have been compared and investigated with the experimental results of the piezocone penetration and dissipation tests. The formulations and the results are described in part 'Ⅰ' and part 'Ⅱ', respectively.

2. Updated Lagrangian Formulation of Constitutive Relations

This section describes the elastoplastic-viscoplastic constitutive relations in the frame of Updated Lagrangian formulation. In this research, the anisotropic elastoplastic-viscoplastic bounding surface model was used. Details on the model are presented in Kaliakin and Dafalias (1990), Al-Shamrani and Sture (1994), and Kim (2000).

Fig. 1 explains that the body occupies a volume V_0, V_n, V_{n+1}, at load increments 0, n, and n+1, respectively, corresponding to time t^0, t^n, and t^{n+1} in the fixed cartesian coordinate system. In the Updated Lagrangian formulation, all quantities in the n+1 configuration are determined with respect to the previous n configuration and the reference configuration is updated after each incremental step. In the following development, the superscript s or 's denote the quantities for the solid skeleton, i.e., the 'effective' concept.

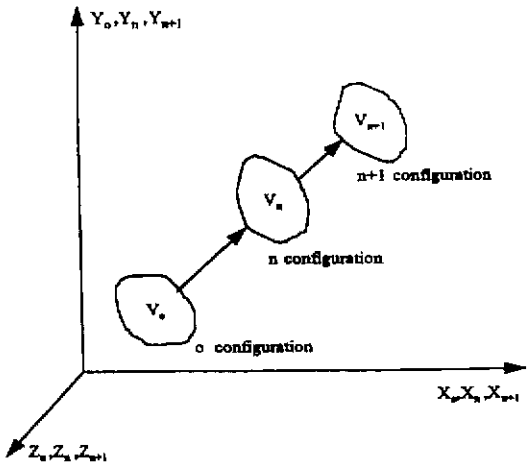

Fig. 1 Configuration of a body

For finite deformations, the elastoplastic-viscoplastic constitutive equations for the solid skeleton are given by

$$\overset{\circ}{\sigma}'_{ab} = D_{abcd} d^s_{cd} - \varphi_{ab} \tag{1}$$

where D is the elastoplastic stress-strain matrix and φ_{ab} is the viscoplastic contribution. The spatial strain rate tensor d is given by

$$d^s_{ac} = \frac{1}{2}\left(v^s_{a,c} + v^s_{c,a}\right) \tag{2}$$

where v^s is velocity of solid particle. The relation between the total corotational stress rate tensor, $\overset{\circ}{\sigma}_{ab}$,and the effective corotational stress rate tensor, $\overset{\circ}{\sigma}'_{ab}$, is expressed using pore water pressure, P_W, as

$$\overset{\circ}{\sigma}_{ab} = \overset{\circ}{\sigma}'_{ab} + \dot{P}_w \delta_{ab} \tag{3}$$

Voyiadjis and Kattan (1989) suggested the effective corotational stress rate tensor, $\overset{\circ}{\sigma}'_{ab}$, as

$$\overset{\circ}{\sigma}'_{ab} = \dot{\sigma}'_{ab} - W^{*s}_{ac}\sigma'_{cd} + W^{*s}_{cb}\sigma'_{ac} \tag{4}$$

$$W^{*s}_{ac} = W^s_{ab} - W^{s*}_{ac} \quad W^s_{ac} = \frac{1}{2}\left(v^s_{a,c} - v^s_{c,a}\right) \tag{5}$$

where $\dot{\sigma}'_{ab}$ is the effective Cauchy stress rate tensor, σ'_{ac} is the effective Cauchy stress tensor, W^{s*}_{ac} is the modified spin tensor, W^{s*}_{ac} is the plastic spin tensor.

The relation between the Cauchy stress tensor, ${}^{n+1}\sigma_{ab}$, and the second Piola-Kirchhoff stress tensor, ${}^{n+1}_{n}S_{AB}$, is given by

$${}^{n+1}\sigma_{ab} = J^{s-1} X^s_{a,A} X^s_{b,B} {}^{n-1}_{n}S_{AB} {}^{n+1}_{n}S_{AB} = J^s X^s_{A,a} X^s_{B,b} {}^{n+1}\sigma_{ab} \tag{6}$$

where J^s is the corresponding Jacobian for the solids and $X^s_{a,A}$ is the deformation gradient expressed as

$$X^s_{a,A} = \frac{\partial Z^s_a}{\partial {}^n X^s_A} = \frac{\partial {}^{n+1}X^s_a}{\partial {}^n X^s_A} \tag{7}$$

By differentiating both sides of the second Piola-Kirchhoff stress tensor in equation (6) with respect to time in the Lagrangian reference frame, the second Piola-Kirchhoff stress rate tensor is obtained as

$$\dot{S}_{AB} = J^s v^s_{C,c} X^s_{A,a} X^s_{B,b} \sigma_{ab} + J^s X^s_{A,a} X^s_{B,b} \dot{\sigma}_{ab} - J^s X^s_{A,c} v^s_{C,a} X^s_{B,b} \sigma_{ab} - J^s X^s_{A,a} X^s_{B,c} v^s_{C,b} \sigma_{ab} \quad (8)$$

where

$$\sigma_{ab} = \sigma'_{ab} + P_w \delta_{ab} \qquad \dot{\sigma}_{ab} = \dot{\sigma}'_{ab} + \dot{P}_w \delta_{ab} \quad (9)$$

By substituting equation (2), equation (4) to equation (5), and equation (9) into equation (8), the following expression is obtained.

$$\dot{S}_{ab} = J^s X^s_{A,a} X^s_{B,b} [\overset{\circ}{\sigma}'_{ab} - d^s_{ac}\sigma'_{cb} - d^s_{bc}\sigma'_{ac} + d^s_{cc}\sigma'_{ab} + \dot{P}_w \delta_{ab} + d^s_{cc} P_w \delta_{ab} - 2d^s_{ab} P_w - W^{s*}_{ac}\sigma'^{s}_{cb} + W^{s*}_{cb}\sigma'^{s}_{ac}] \quad (10)$$

where the spatial strain rate tensor, d^s is related to the material strain rate tensor, $\dot{\varepsilon}^s$, by

$$d^s_{cd} = X^s_{c,C} X^s_{d,D} \dot{\varepsilon}^s_{CD} \quad (11)$$

Now, substituting the elastoplastic-viscoplastic constitutive relation, equation (1), into equation (10) together with equation (11), and neglecting the plastic spin tensor yields

$$\dot{S}_{ab} = D^*_{ABCD} \dot{\varepsilon}_{CD} + J^s X^s_{A,a} X^s_{B,b} \dot{P}_w \delta_{ab} - J^s X^s_{A,a} X^s_{B,b} \varphi_{ab} \quad (12)$$

where

$$D^*_{ABCD} = [D_{ABCD} - \sigma'^{s}_{cb}\delta_{ad} - \sigma'^{s}_{ac}\delta_{bd} + \sigma'^{s}_{ab}\delta_{cd} + \dot{P}_w \delta_{ab}\delta_{cd} - 2P_w \delta_{ac}\delta_{bd}](J^s X^s_{A,a} X^s_{B,b} X^s_{C,c} X^s_{D,d}) \quad (13)$$

The last term in equation (12) is the viscoplastic contribution.

3. Updated Lagrangian Formulation of Virtual Work Equation and Theory of Mixtures

This section describes the theory of mixtures and how the form of the virtual work equation changes due to the viscoplastic contribution. Accordingly, the finite element formulation changes and it is described in the following section.

The virtual work equation in the updated Lagrangian formulation is given by (Bathe, 1990)

$$\int_{{}^nV} {}^{n+1}_{n}S_{AB}\,\delta\left({}^{n+1}_{n}\varepsilon_{AB}\right) d^nV = {}^{n+1}R \quad (14)$$

where ${}^{n+1}R$ is the external virtual work due to the applied loads and surface tractions, and it is expressed, when the external virtual work is deformation independent,

$${}^{n+1}R = \int_{V^0} {}^{n+1}b_i \delta u^s_i dV^0 + \int_{S^0} {}^{n+1}t_k \delta u^s_k dS^0 \quad (15)$$

when the external virtual work is deformation dependent,

$${}^{n+1}R = \int_{V^{n+1}} {}^{n+1}b_i \delta u^s_i dV^{n-1} + \int_{S^{n+1}} {}^{n+1}t_k \delta u^s_k dS^{n+1} \quad (16)$$

where b is the body force, δu is the variation of the displacement, t is the surface loading, V is the volume, ${}^{n+1}_{n}\varepsilon$ is the total strain, and it is decomposed into the linear strain, ${}_n e_{AB}$, and the nonlinear strain, ${}_n\eta_{AB}$.

$${}^{n+1}_{n}\varepsilon = {}_n e_{AB} + {}_n\eta_{AB} \quad (17)$$

$${}_n e_{AB} = \frac{1}{2}({}_n u_{A,B} + {}_n u_{B,A}) \qquad {}_n\eta_{AB} = \frac{1}{2}({}_n u_{K,A} + {}_n u_{K,B}) \quad (18)$$

where u is the displacement vector.

The ${}^{n+1}_{n}S_{AB}$ is the second Piola-Kirchhoff stress tensor at n+1 referred to the n configuration as indicated in fig. 1 and it is related to the Cauchy stress tensor, ${}^n\sigma_{AB}$, by

$${}^{n+1}_{n}S_{AB} = {}^n\sigma_{AB} + {}^n\Delta S_{AB} \quad (19)$$

where ${}^n\Delta S_{AB}$ is the incremental stress tensor from con figuration n to n+1 and the total Cauchy stress tensor, ${}^n\sigma_{AB}$, has the following relation with the effective Cauchy stress tensor, ${}^n\sigma'_{AB}$,

$$ {}^{n}\sigma_{AB} = {}^{n}\sigma'_{AB} + P_w \delta_{AB} \tag{20} $$

By substituting equation (17) and equation (19) into equation (14), the left side of the virtual equation is expressed as

$$ \begin{aligned} &\int_{{}^{n}V} {}_{n}^{n+1}S_{AB}\,\delta\left({}_{n}^{n+1}\varepsilon_{AB}\right) d^{n}V \\ &= \int_{{}^{n}V} \left({}^{n}\sigma_{AB} + \Delta_n S_{AB}\right) \delta\left({}_{n}e_{AB} + {}_{n}\eta_{AB}\right)\, d^{n}V \\ &= \int_{{}^{n}V} {}^{n}\sigma_{AB}\,\delta\left({}_{n}e_{AB} + {}_{n}\eta_{AB}\right) d^{n}V \\ &+ \int_{{}^{n}V} \Delta_n S_{AB}\,\delta\left({}_{n}e_{AB} + {}_{n}\eta_{AB}\right) d^{n}V \end{aligned} \tag{21} $$

Using equation (12), $\Delta_n S_{AB}$ can be expressed as

$$ \begin{aligned} \Delta_n S_{AB} &= \int_{t}^{t+\Delta t} \dot{S}_{AB}\, dt \\ &= D^{-}_{ABCD} \int_{t}^{t+\Delta t} \dot{\varepsilon}_{CD}\, dt + J^{s} X^{s}_{A,a} X^{s}_{B,b} \\ &\quad \int_{t}^{t+\Delta t} \dot{P}_w\, dt - J^{s} X^{s}_{A,a} X^{s}_{B,b} \varphi_{ab} \\ &= \mathrm{D}^{*}_{ABCD} \Delta\varepsilon_{CD} + \mathrm{J}^{s}\mathrm{X}^{s}_{A,a}\mathrm{X}^{s}_{B,b}\Delta\mathrm{P}_w - \mathrm{J}^{s}\mathrm{X}^{s}_{A,a}\mathrm{X}^{s}_{B,b}\varphi_{ab} \end{aligned} \tag{22} $$

By substituting equation (22) into equation (21), and by ignoring the term that contains $\eta\delta\eta$, since it is very small for finite strains, the following virtual work equation is obtained.

$$ \begin{aligned} &\int_{{}^{n}V} \mathrm{D}^{*}_{ABCD}\left(\Delta_n e_{CD} + \Delta_n \eta_{CD}\right) \delta_n e_{AB}\, dV^{n} \\ &+ \int_{{}^{n}V} \mathrm{D}^{*}_{ABCD} \Delta_n e_{CD} \delta_n \eta_{AB}\, dV^{n} \\ &+ \int_{{}^{n}V} \left({}^{n}\dot{\sigma}_{AB} + {}^{n}\mathrm{P}_w \delta_{AB}\right) \delta_n \eta_{AB}\, dV^{n} \\ &+ \int_{{}^{n}V} \mathrm{J}^{s}\mathrm{X}^{s}_{A,a}\mathrm{X}^{s}_{B,b}\delta_{ab}\Delta\mathrm{P}_w\left(\delta_n e_{AB} + \delta_n \eta_{AB}\right) dV^{n} \\ &+ \int_{{}^{n}V} \mathrm{J}^{s}\mathrm{X}^{s}_{A,a}\mathrm{X}^{s}_{B,b}\varphi_{ab}\left(\delta_n e_{AB} + \delta_n \eta_{AB}\right) dV^{n} \\ &= {}^{n+1}\mathrm{R} - \int_{{}^{n}V} \left({}^{n}\sigma'_{AB} + {}^{n}\mathrm{P}_w \delta_{AB}\right) \delta_n e_{AB}\, dV^{n} \end{aligned} \tag{23} $$

Equation (23) is a form of elastoplastic-viscoplastic virtual work equation. The last term of the left side in the equation indicates the viscoplastic contribution. Equation (23) is implemented into a finite elemet formulation as the first coupled equation. The finite element formulation also changes due to the change of the virtual work equation.

Theory of mixtures was used to explain the behavior of soils as a multiphase medium (Prevost, 1980). In theory of mixtures, soil is considered as a mixture of multiphase deformable medium of solid grains and water when saturated. Solid grain and water are respectively regarded as a continuum and follows its own motion. Fig. 2 shows the schematic of theory of mixtures for the saturated case. The final coupled equation in theory of mixtures is derived using the law of conservation of mass and a certain flow law of water through the voids.

The coupled equation in theory of mixtures in the Updated Lagrangian formulation is obtained as (Kiousis, et al., 1988; Voyiadjis and Abu-Farsakh, 1997)

$$ \begin{aligned} &J^{s} C^{s^{-1}}_{ij}\, \dot{\varepsilon}_{ij} - J^{s} C^{s^{-1}}_{ij} C^{s^{-1}}_{ij} X^{s}_{D,a} \frac{\partial}{\partial X_D} \\ &\left[\frac{n^{w}}{\gamma^{w}} K^{ws}_{AB} X^{s}_{a,A}\left(\frac{\partial P_w}{\partial X_B} - \rho_w B_B\right)\right] = 0 \end{aligned} \tag{24} $$

where

$$ \mathrm{C}^{s}_{ij} = \mathrm{X}^{s}_{k,i}\mathrm{X}^{s}_{k,j} \qquad \mathrm{b}_b = \mathrm{X}^{s}_{b,B}\mathrm{B}_B \tag{25} $$

The b is the body force vector, K^{ws} is the permeability tensor in m/sec, γ_w is the unit weight of the water, and ρ_w is the intrinsic mass density of the water. The soil porosity, n^w, is updated from at n configuration to at n+1 configuration

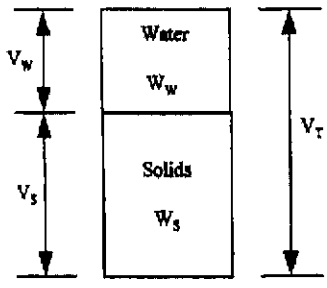

Fig. 2 Representation of soil as two-phase medium

using the jaccobian of solid grains, J^s.

$$\frac{1-n^w_{n+1}}{1-n^w_n}=\frac{1}{J^s} \tag{26}$$

Equation (24) is implemented into a finite element formulation as the second coupled equation together with the first coupled equation (23).

4. Finite Element Formulation

This section describes and interprets the implementation of the first and the second coupled equations into a finite element formulation.

The following finite element discretization is used for the displacement, u, and the pore water pressure, Pw.

$$u=\mathbf{h}\cdot U \quad P_w=\mathbf{N}\cdot W \quad \frac{\partial P_w}{\partial X_B}=\mathbf{N}_{,B}W \tag{27}$$

where **h** is the displacement shape function, **N** is the pore water pressure shape function which is different from the displacement shape function, U is the nodal displacement, and W is the nodal pore water pressure.

The variation of linear and nonlinear strains are given by

$$\delta e=\mathbf{B}_L\cdot\delta U \quad \delta\eta=\mathbf{B}_{NL}\cdot\delta U \tag{28}$$

Where $\mathbf{B}_L$ and $\mathbf{B}_{NL}$ are the linear and nonlinear strain-displacement matrices. Substituting equation (28) into the first coupled equation (23) yields

$$\delta U^T\left({}_n\mathbf{K}_L+{}_n\mathbf{K}_{NM}+{}_n\mathbf{K}^T_{NL}+{}_n\mathbf{K}^s\right)\Delta U-\delta U^T\,{}^n\mathbf{\Omega}\Delta W=\delta U^T\,{}_n\mathbf{\Phi} \tag{29}$$

Equation (29) is valid for any virtual displacement δU^T; therefore, the following expression is obtained

$${}_n\mathbf{K}\Delta U+{}^n\mathbf{\Omega}\Delta W={}_n\mathbf{\Phi} \tag{30}$$

Equation (30) is the final form of the numerical formulation of the first coupled equation (23).

In equation (30), the elastoplastic stiffness matrix, nK, is expressed as

$${}_n\mathbf{K}={}_n\mathbf{K}_L+{}_n\mathbf{K}_{NL}+{}_n\mathbf{K}^T_{NL}+{}_n\mathbf{K}^s \tag{31}$$

$${}_n\mathbf{K}_L=\int_{{}^nV}{}_n\mathbf{B}^T_L\cdot\mathbf{D}^*\cdot{}_n\mathbf{B}_L\,d^nV$$

$${}_n\mathbf{K}_{NL}=\int_{{}^nV}{}_n\mathbf{B}^T_L\cdot\mathbf{D}^*\cdot{}_n\mathbf{B}_{NL}\,d^nV \tag{32}$$

$${}_n\mathbf{K}^s=\int_{{}^nV}{}_n\mathbf{C}_{NL}\,d^nV \quad {}_n\mathbf{C}_{NL}={}_n\mathbf{B}^{*T}_{NL}\cdot{}^n\sigma\cdot{}_n\mathbf{B}^*_{NL} \tag{33}$$

where ${}_n\mathbf{K}_L$ is the linear stiffness matrix, ${}_n\mathbf{K}_{NL}$ is the nonlinear matrix. ${}_n\mathbf{K}^s$ is the nonlinear geometric stiffness matrix, and ${}_n\mathbf{C}_{NL}$ is the nonlinear matrix.

The coupling matrix, ${}_n\mathbf{\Omega}$, in equation (30) is expressed as

$${}_n\mathbf{\Omega}=\int_{{}^nV}J^sX^s_{A,a}X^s_{B,b}\left({}_n\mathbf{B}^T_L+{}_n\mathbf{B}^T_{NL}\right)\overline{\mathbf{N}}_{ab}d^nV$$

$$\overline{\mathbf{N}}=\mathbf{mN} \tag{34}$$

where

$$\begin{aligned}&\mathbf{m}^T=\{1\ 1\ 0\} \text{ for two dimension}\\&\mathbf{m}^T=\{1\ 1\ 1\ 0\ 0\ 0\} \text{ for three dimension}\end{aligned} \tag{35}$$

such that

$$\sigma=\sigma'+\mathrm{m}\,\mathrm{Pw} \tag{36}$$

In equation (30),

$$\mathbf{\Phi}={}^{n+1}\mathbf{R}-\int_{{}^nV}{}_n\mathbf{B}^T_L\cdot{}^n\sigma dV^n+\int_{{}^nV}J^sX^s_{A,a}X^s_{B,b}\varphi_{ab}\left({}_n\mathbf{B}^T_L+{}_n\mathbf{B}^T_{NL}\right)dV^n \tag{37}$$

In equation (37), the last term in the right side indicates the viscoplastic contribution. With equation (31) through equation (37), the numerical formulation of the first coupled equation (30) is completely defined.

The condition that the continuity equation (24), the second coupled equation, applies throughout the continuum using Galerkin's weighed residual method requires that

$$\int_{{}^nV}\left\{J^sC^{s^{-1}}_{ij}\dot{\varepsilon}_{ij}-J^sC^{s^{-1}}_{ij}C^{s^{-1}}_{ij}\frac{\partial}{\partial X_A}\left[\frac{n^w}{\gamma_n}K^{ws}_{AB}\left(\frac{\partial P_w}{\partial X_B}-\rho B_B\right)\right]\right\}\overline{P}_w d^nV=0 \tag{38}$$

By applying Green's theory, the weak form of equation (38) is obtained as

$$\int_{{}^{n}V} J^{s} C_{ij}^{s-1} \dot{\varepsilon}_{ij} \bar{P}_{w} d^{n}V - \int_{{}^{n}V} \frac{n^{w}}{\gamma_{w}} J^{s} C_{RS}^{s-1} C_{RS}^{s-1} K_{AB}^{ws}$$

$$\left(\frac{\partial P_{w}}{\partial X_{B}} + \rho B_{B} \right) \frac{\partial \bar{P}_{w}}{\partial X_{B}} d^{n}V - \int_{{}^{n}S} q_{n} \bar{P}_{w} d^{n}V = 0 \qquad (39)$$

where the weighted residual (virtual pore pressure), $\bar{P}_{w}$, the pressure gradient, $\partial \bar{P}_{A} / \partial X_{B}$, are given by

$$\bar{P}_{w} = \mathbf{N} \bar{w} \quad \frac{\partial \bar{P}_{w}}{\partial X_{A}} = \mathbf{N}_{,A} \bar{w} \qquad (40)$$

In equation (39), q_n is the seepage velocity normal to the boundary surface. By substituting equation (29), equation (30), and equation (40) into equation (39), the final form of the numerical formulation of the second coupled equation is obtained as

$$-{}_{n}\mathbf{\Omega}^{T} \Delta U + {}_{n}\mathbf{\Psi} \delta t \Delta W = {}_{n}\mathbf{\Pi} \qquad (41)$$

where

$${}_{n}\mathbf{\Psi} = \int_{{}^{n}V} J^{s} \frac{n^{w}}{\gamma_{w}} C_{ij}^{s-1} C_{ij}^{s-1} {}_{n}K_{AB}^{ws} N_{,A} N_{,B} d^{n}V \qquad (42)$$

$${}_{n}\mathbf{\Pi} = \delta t \mathbf{G} - \delta t {}_{n}\mathbf{\Psi} W^{n} - \int_{{}^{n}S} q_{n} \bar{P}_{w} d^{n}A \qquad (43)$$

$$\mathbf{G} = -\int_{{}^{n}V} J^{s} n^{w} C_{ij}^{s-1} C_{ij}^{s-1} {}_{n}K_{AB}^{ws} N_{,A} N_{,B} d^{n}V \qquad (44)$$

$$\Delta U = U^{n+1} - U^{n} \quad \Delta W = W^{n+1} - W^{n} \qquad (45)$$

where ΔU is the incremental nodal displacement and ΔW is the incremental nodal excess pore water pressure.

By assembling the numerical form of the first coupled equation (30) and the numerical form of the second coupled equation (41), the global coupled expression for the behavior of the two-phase skeleton-fluid state is obtained as

$$\begin{bmatrix} {}_{n}\mathbf{K} & -{}_{n}\mathbf{\Omega} \\ -{}_{n}\mathbf{\Omega}^{T} & -\delta t {}_{n}\mathbf{\Psi} \end{bmatrix} \begin{Bmatrix} \Delta U \\ \Delta W \end{Bmatrix} = \begin{Bmatrix} {}_{n}\mathbf{\Phi} \\ {}_{n}\mathbf{\Pi} \end{Bmatrix} \qquad (46)$$

To define the elements of the matrices of the global coupled equation (46), the 8-noded isoparametric plane strain element is used.

The shape function for the 8-noded isoparametric plane element is given by

$$\mathbf{h} =$$

$$\begin{bmatrix} h_1 & 0 & h_2 & 0 & h_3 & 0 & h_4 & 0 & h_5 & 0 & h_6 & 0 & h_7 & 0 & h_8 & 0 \\ 0 & h_1 & 0 & h_2 & 0 & h_3 & 0 & h_4 & 0 & h_5 & 0 & h_6 & 0 & h_7 & 0 & h_8 \end{bmatrix} \qquad (47)$$

The element displacements are related to the nodal displacements through the shape function h as

$$u_{i} = \sum_{k=1}^{8} \mathbf{h}_{k} u_{i}^{(k)} \qquad (48)$$

The shape functions in equation (48) are expressed in terms of local coordinates, so the chain rule is used to refer the displacement derivatives in terms of the global coordinates. The displacement derivatives with respect to the global coordinates are given by (Bathe, 1990)

$$\frac{\partial u_{i}}{\partial {}^{n}X_{j}} = \sum_{k=1}^{8} \frac{\partial u_{i}}{\partial {}^{n}X_{j}} U^{(k)} \qquad (i=1,2;j=1,2),$$

$$\frac{\partial \mathbf{h}_{k}}{\partial {}^{n}X_{j}} = \mathbf{J}_{j1}^{-1} \frac{\partial \mathbf{h}_{k}}{\partial {}^{n}r} + \mathbf{J}_{j2}^{-1} \frac{\partial \mathbf{h}_{k}}{\partial {}^{n}s} \qquad (49)$$

Using equation (49), the deformation gradient matrix F for the incremental displacement is obtained as

$$F = \left\{ \frac{\partial u_{i}}{\partial {}^{n}X_{j}} \right\} = \begin{bmatrix} \frac{\partial u_{1}}{\partial {}^{n}X_{1}} & \frac{\partial u_{1}}{\partial {}^{n}X_{2}} \\ \frac{\partial u_{2}}{\partial {}^{n}X_{1}} & \frac{\partial u_{2}}{\partial {}^{n}X_{2}} \end{bmatrix} \qquad (50)$$

Using equation (50) and equation (28), the linear strain-displacement matrix, B_L, and the nonlinear strain-d isplacement matrix, B_{NL}, is obtained by

$$[\mathbf{B}_{L}] =$$

$$\begin{bmatrix} {}^{n}h_{1,1} & 0 & {}^{n}h_{2,1} & 0 & {}^{n}h_{3,1} & \cdots & {}^{n}h_{7,1} & 0 & {}^{n}h_{8,1} & 0 \\ 0 & {}^{n}h_{1,2} & 0 & {}^{n}h_{2,2} & 0 & \cdots & 0 & {}^{n}h_{7,2} & 0 & {}^{n}h_{8,2} \\ {}^{n}h_{1,2} & {}^{n}h_{1,1} & {}^{n}h_{2,2} & {}^{n}h_{2,1} & {}^{n}h_{3,2} & \cdots & {}^{n}h_{7,2} & {}^{n}h_{7,1} & {}^{n}h_{8,2} & {}^{n}h_{8,1} \end{bmatrix} \qquad (51)$$

$$\mathbf{B}_{NL} = \mathbf{G} \cdot \mathbf{Q} \cdot \mathbf{H} \qquad (52)$$

where

$$[\mathbf{G}] = \begin{bmatrix} {}^{n}h_{1,1} & 0 & {}^{n}h_{1,1} & 0 & {}^{n}h_{2,1} & \cdots & {}^{n}h_{8,1} & 0 & {}^{n}h_{8,1} & 0 \\ 0 & {}^{n}h_{1,2} & 0 & {}^{n}h_{1,2} & 0 & \cdots & 0 & {}^{n}h_{8,2} & 0 & {}^{n}h_{8,2} \\ {}^{n}h_{1,2} & {}^{n}h_{1,1} & {}^{n}h_{1,2} & {}^{n}h_{1,1} & {}^{n}h_{2,2} & \cdots & {}^{n}h_{8,2} & {}^{n}h_{8,1} & {}^{n}h_{8,2} & {}^{n}h_{8,1} \end{bmatrix} \tag{53}$$

$$[\mathbf{Q}]^{T} = \begin{bmatrix} {}^{n}u_1^1 & 0 & 0 & 0 & {}^{n}u_1^2 & 0 & \cdots & {}^{n}u_1^8 & 0 & 0 & 0 \\ 0 & {}^{n}u_1^1 & 0 & 0 & 0 & {}^{n}u_1^{21} & \cdots & 0 & {}^{n}u_1^8 & 0 & 0 \\ 0 & 0 & {}^{n}u_2^1 & 0 & 0 & 0 & \cdots & 0 & 0 & {}^{n}u_2^8 & 0 \\ 0 & 0 & 0 & {}^{n}u_2^1 & 0 & 0 & \cdots & 0 & 0 & 0 & {}^{n}u_2^8 \end{bmatrix} \tag{54}$$

$$[\mathbf{H}] = \begin{bmatrix} {}^{n}h_{1,1} & 0 & {}^{n}h_{2,1} & 0 & \cdots & {}^{n}h_{7,1} & 0 & {}^{n}h_{8,1} & 0 \\ {}^{n}h_{1,2} & 0 & {}^{n}h_{2,2} & 0 & \cdots & {}^{n}h_{7,2} & 0 & {}^{n}h_{8,2} & 0 \\ 0 & {}^{n}h_{1,1} & 0 & {}^{n}h_{2,1} & \cdots & 0 & {}^{n}h_{7,1} & 0 & {}^{n}h_{8,1} \\ 0 & {}^{n}h_{1,2} & 0 & {}^{n}h_{2,2} & \cdots & 0 & {}^{n}h_{7,2} & 0 & {}^{n}h_{8,2} \end{bmatrix} \tag{55}$$

As shown in equation (33), the nonlinear matrix, nC_{NL}, is expressed as

$$[{}_{n}\mathbf{C}_{NL}] = [{}_{n}\mathbf{B}^{*}_{NL}]^{T} [{}^{n}\boldsymbol{\sigma}] [{}_{n}\mathbf{B}^{*}_{NL}] \tag{56}$$

The geometric nonlinear strain-displacement matrix, $[{}_{n}\mathbf{B}^{*}_{NL}]$, is rearranged in the following form

$$[\mathbf{B}^{*}_{NL}] = \begin{bmatrix} {}^{n}h_{1,1} & 0 & {}^{n}h_{2,1} & 0 & \cdots & {}^{n}h_{7,1} & 0 & {}^{n}h_{8,1} & 0 \\ {}^{n}h_{1,2} & 0 & {}^{n}h_{2,2} & 0 & \cdots & {}^{n}h_{7,2} & 0 & {}^{n}h_{8,2} & 0 \\ 0 & {}^{n}h_{1,1} & 0 & {}^{n}h_{2,1} & \cdots & 0 & {}^{n}h_{7,1} & 0 & {}^{n}h_{8,1} \\ 0 & {}^{n}h_{1,2} & 0 & {}^{n}h_{2,2} & \cdots & 0 & {}^{n}h_{7,2} & 0 & {}^{n}h_{8,2} \end{bmatrix} \tag{57}$$

The stress tensor is given by

$$[{}^{n}\boldsymbol{\sigma}] = \begin{bmatrix} {}^{n}\sigma_{11} & {}^{n}\sigma_{12} & 0 & 0 \\ {}^{n}\sigma_{21} & {}^{n}\sigma_{22} & 0 & 0 \\ 0 & 0 & {}^{n}\sigma_{11} & {}^{n}\sigma_{12} \\ 0 & 0 & {}^{n}\sigma_{21} & {}^{n}\sigma_{22} \end{bmatrix} \tag{58}$$

The global coupled equation (46) obtained from the first and the second coupled equations is now completely defined with equation (47) through equation (58).

5. Summary and Conclusions

In this research, the anisotroic elastoplastic-viscoplastic bounding surface model has been formulated in the Updated Lagrangian reference frame to consider the large strain nature of the piezocone penetration. Virtual work equation and finite element equations have been also formulated in the Updated Lagrangian reference frame. Theory of mixtures formulated in the Updated Lagrangian reference frame has been incorporated to explain the behavior of soils as a multiphase medium. It has been observed that the viscoplastic part of the soil model affected the whole formulations, namely, the Updated Lagrangian formulation and corresponding finite element formulation. The results of the finite element analyses are compared with the experimental results of the piezocone penetration and dissipation tests in part 'II'.

Acknowledgments

The financial support for the work described in this paper was provided through a grant CMS-9531782 by NSF. The writer acknowledges Professor Mehmet T. Tumay, Professor George Z. Voyiadjis, and Dr. Abu-Farsakh.

References

1. Abu-Farsakh, M. Y., Voyiadjis, G. Z., and Tumay, M. T. (1997), "Numerical Analysis of the Miniature Piezocone Penetration Tests (PCPT) in Cohesive Soils." International Journal for Numerical and Analytical Methods on Geomechanics (In Press)
2. Al-Shamrani, M. A. and Sture, S. (1994), "Characterization of Time-dependent Behavior of Anisotropic Cohesive Soils," Computer Methods and Advances in Geomechanics, Siriwardane & Zaman (eds), pp. 505-511
3. Bathe, K. J. (1990), Finite Element Procedures in Engineering Analysis, Prentice-Hall, Inc., New Delhi, India
4. De Borst, R. and Vermeer, P. A. (1984), "Possibilities and Limitations of Finite Element for Limit Analysis," Geotechnique, Vol. 34, No. 2, pp. 199-210
5. Kaliakin, V. N. and Dafalias, Y. F. (1990), "Theoretical Aspects of the Elastoplastic-Viscoplastic Bounding Surface Model for Cohesive

Soils," Japanese Society of Soil Mechanics and Foundations Engineering, Vol. 30, No. 3, pp. 11-24.

6. Kim. D.-K. (2000), "A Study on the Model Parameters of the Anisotropic Elastoplastic-viscoplastic Bounding Surface Model for Cohesive Soils," Journal of the Korean Geotechnical Society Vol. 17, No. 3
7. Kiousis, P. D., Voyiadjis, G Z., and Tumay, M. T. (1988), "A Large Strain Theory and Its Application in the Analysis of the Cone Penetration Mechanism," International Journal for Numerical and Analytical Methods in Geomechanics, Vol. 12, pp. 45-60.
8. Prevost, J. H. (1980), "Mechanics of Continuous Porous Media," International Journal of Engineering Science, Vol. 18, pp. 787-800
9. Sandven, R. (1990), "Strength and Deformation Properties of fine grained Soils obtained from Piezocone Tests," Ph. D. Dissertation, The Department of Civil Engineering, The Norwegian Institute of Technology
10. Teh, C. I. and Houlsby, G T. (1991), "An Analytical Study of the Cone Penetration Test in Clay," Geotechnique, Vol 41, No. 1, pp. 17-34
11. Van den Berg, P., Teunissen, J.A M., and Huetink, J. (1994), "Cone Penetration in Layered Media, an ALE Finite Element Formulation," Proceedings of 8th IACMAG, West Virginia. USA, in "Computer Methods and Advances in Geomechanics', Siriwardane and Zaman (eds), Balkema, Rotterdam, May, pp 1957-1962
12. Voyiadjis, G Z. and Abu-Farsakh, M. Y. (1997), "Coupled Theory of Mixtures for Clayey Soils." Computers and Geotechnics, Vol. 20, No. $\frac{3}{4}$, pp. 195-222
13. Voyiadjis, G. Z. and Kattan, P. I. (1989), "Eulerian Constitutive Model for Finite Deformation Plasticity with Anisotropic Hardening," Mechanics of Materials, Vol. 7, pp. 279-293.

(접수일자 2000. 5. 10)